Electronic Supplementary Information (ESI)

Adsorption Structure Determination of a Large Polyaromatic Trithiolate on Cu(111): Combination of LEED-I(V) and DFT-vdW†

Thomas Sirtl,[a] Jelena Jelic,[b] Jörg Meyer,[b] Kalpataru Das,[c] Wolfgang M. Heckl,[a,d] Wolfgang Moritz,[e] John Rundgren,[f] Michael Schmittel,[c] Karsten Reuter,[b] and Markus Lackinger[a,d,]*

[a] Department of Physics, Technische Universität München,
James-Franck-Str. 1, 85748 Garching, Germany and
Center for NanoScience (CeNS), Schellingstr. 4, 80799 Munich, Germany
[b] Department of Chemistry, Technische Universität München, Lichtenbergstr. 4, 85747 Garching, Germany
[c] Center of Micro- and Nanochemistry and Engineering, Organische Chemie I, Universität Siegen, Adolf-Reichwein-Str. 2, 57068 Siegen, Germany
[d] Deutsches Museum, Museumsinsel 1, 80538 Munich, Germany
[e] Department of Earth and Environmental Sciences, Ludwig-Maximilians-University, Theresienstr. 41, 80333 Munich, Germany
[f] Department of Theoretical Physics, KTH Royal Institute of Technology, SE-106 91 Stockholm, Sweden
* *E-mail: markus@lackinger.org; www.2d-materials.com*

Table Of Contents

Experimental Details Low-Energy-Electron-Diffraction

Low-Energy-Electron-Diffraction (LEED) experiments were carried out under ultra-high vacuum (UHV) conditions with a base pressure below 1×10^{-10} mbar. A SPECTALEED 4-grid optics (Omicron NanoTechnology GmbH) was used in combination with an ErLEED digital electronics (SPECS Surface Nano Analysis GmbH). During LEED experiments the sample was cooled to approximately 50 K. LEED-I(V) videos were recorded with a SensiCam CCD camera (PCO AG).

The software package EE2010 (Dr. Michael F. Opheys, http://www.ee2000.de/) was used for data acquisition and extraction of I(V) curves. Structure optimization by dynamic LEED calculations was performed with the home written LEEDFIT software.[1-3]

Cu(111) single crystal surfaces were prepared by cycles of Ar^+ ion sputtering at 2 keV and subsequent e-beam annealing at 820 K for 15 min. The synthesis of TMB and monolayer deposition is described elsewhere.[4]

Calculational Details Density Functional Theory

All density functional theory (DFT) calculations were performed with the plane-wave based code CASTEP[5] using library ultrasoft pseudopotentials[6] and the generalized gradient approximation (GGA) functional due to Perdew, Burke, and Ernzerhof (PBE)[7] to treat electronic exchange and correlation. Long-range dispersive interactions were included on a semi-empirical level through the dispersion-correction scheme suggested by Tkatchenko and Scheffler.[8]

The molecule-surface system was modeled in supercell geometries, using four layer thick Cu slabs (at optimized PBE lattice constant of 3.626 Å), a vacuum region exceeding 20 Å, and a $(3\sqrt{3}\times3\sqrt{3})$ surface unit-cell. Full geometry optimizations of the two topmost slab layers and all molecular degrees of freedom were performed with the BFGS algorithm[8] implemented in CASTEP with a default convergence threshold on the maximum absolute ionic-force component of 0.05 eV/Å. In the initial screening of adsorption sites some of the geometry optimizations were stopped when the last geometry steps led to energetic improvements on the order of 10 meV and it became clear that the structure would be far less favorable than the best adsorption site models tested. At the employed plane-wave kinetic-energy cutoff of 450 eV and reciprocal space integration using (2×2×1) Monkhorst-Pack grids[9] the relative energies of the different optimized structures were converged within 0.05 eV.

Gas phase molecules – the protonated trithiol and the fully deprotonated trithiolate – were also treated in supercell geometries. In order to model “isolated“ molecules, a orthorhombic unit cell of (20×30×20 Å) dimension with Γ-point sampling and the same plane-wave kinetic-energy cutoff of 450 eV was employed.

Constraints for LEED-I(V) Structure Optimization

Supplementary Table S1 Constraints for intramolecular bonds in the trithiolate as used for the initial LEED-I(V) structure optimization.

atoms	distance / pm		
	minimum	maximum	optimum
C→C, next neighbor	140	170	154
C→C, next nearest neighbor	250	280	267
C→C, diagonal	280	320	308
C→S, next neighbor	160	200	181
C→S, next nearest neighbor	270	310	290
C→H, next neighbor	100	130	115
C→H, next nearest neighbor	210	250	233

Experimental vs. Calculated I(V)-Curves

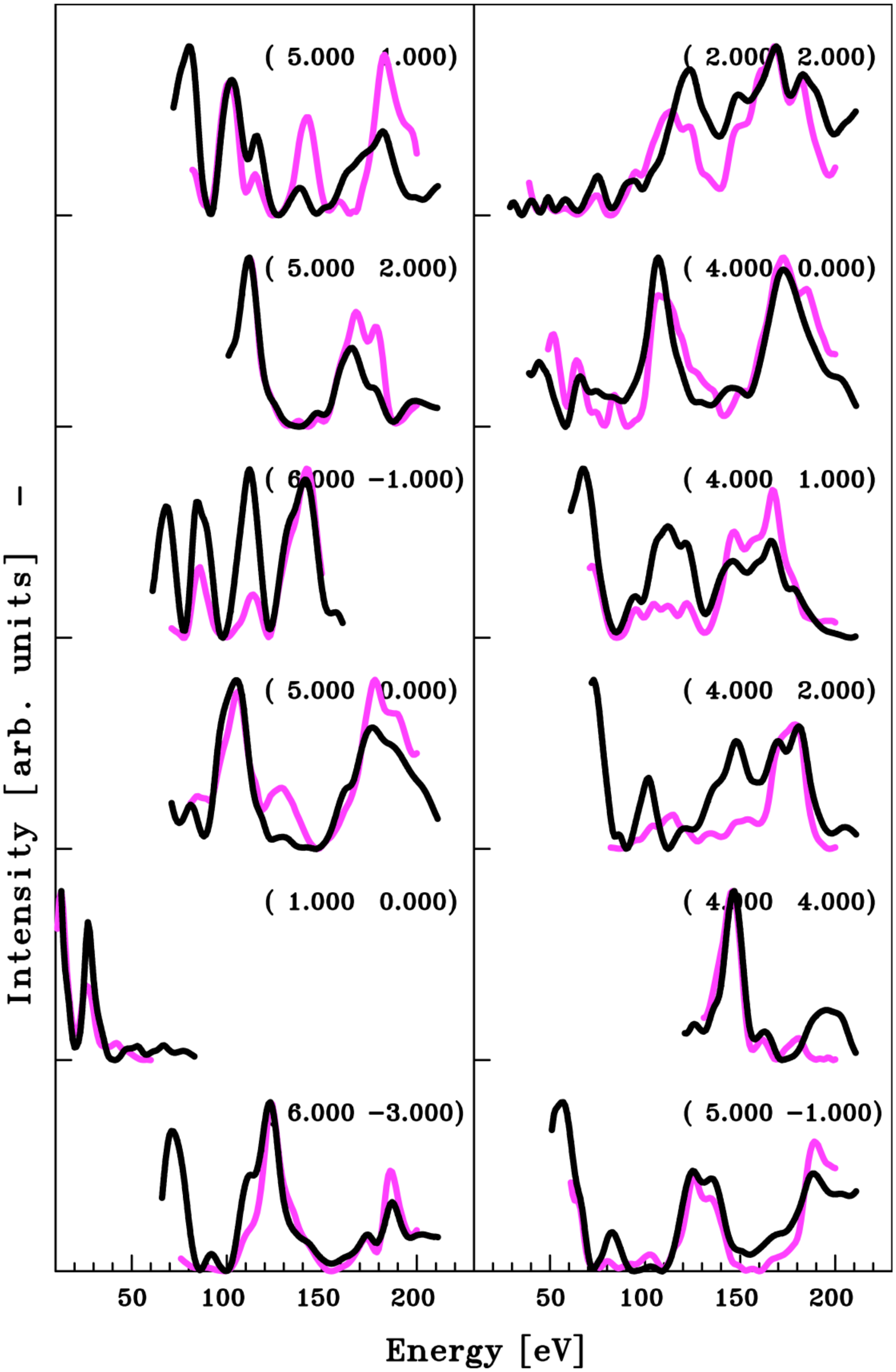

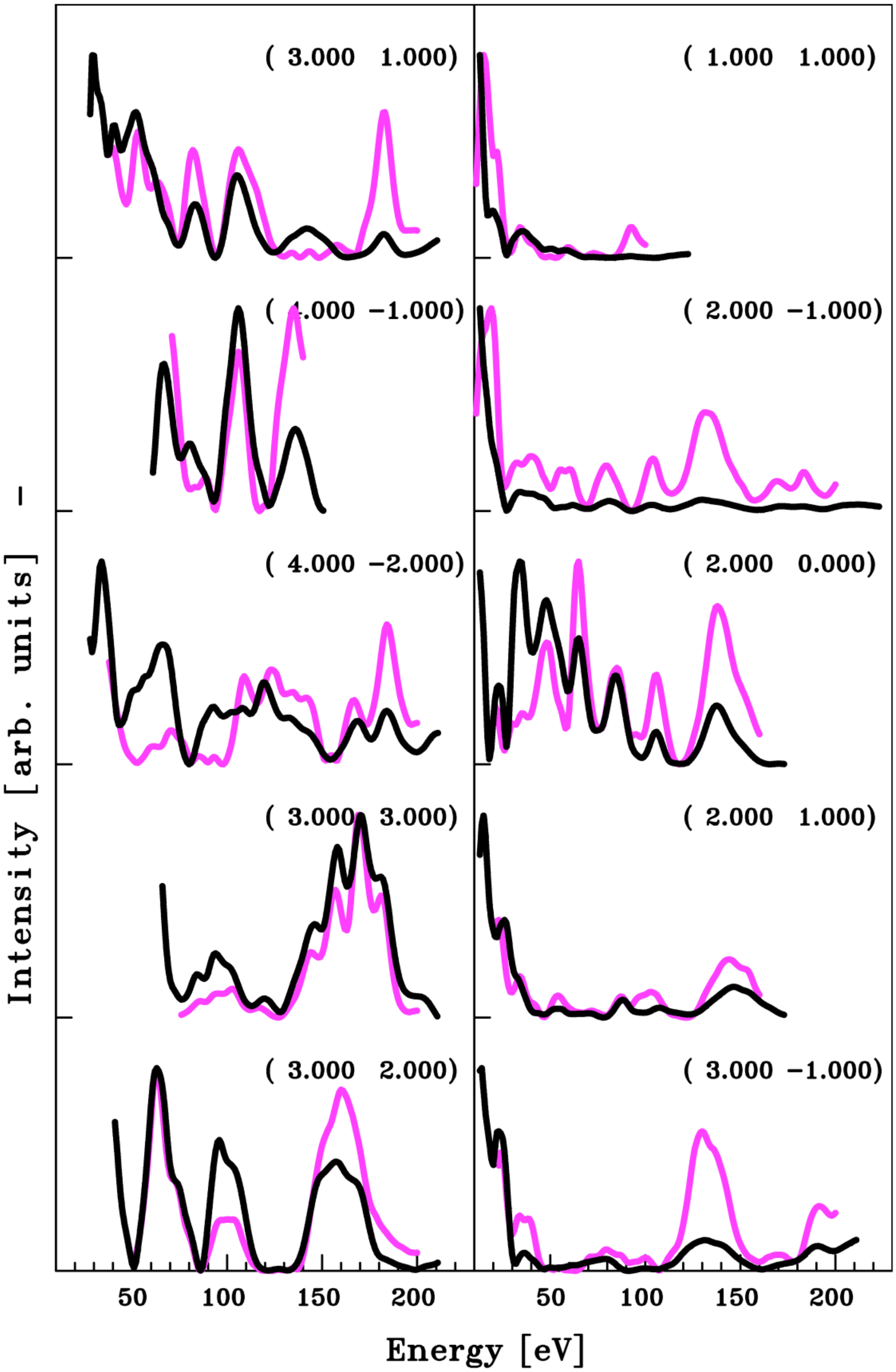

Supplementary Fig. S1 Experimental vs. calculated I(V) curves. Complete dataset of 22 independent experimental (pink) and calculated (black) LEED-I(V) curves for the best-fit model (S: fcc, phenyl: hcp), offset for clarity. Indices are given in brackets.

LEED Optimization Results for Competing Models

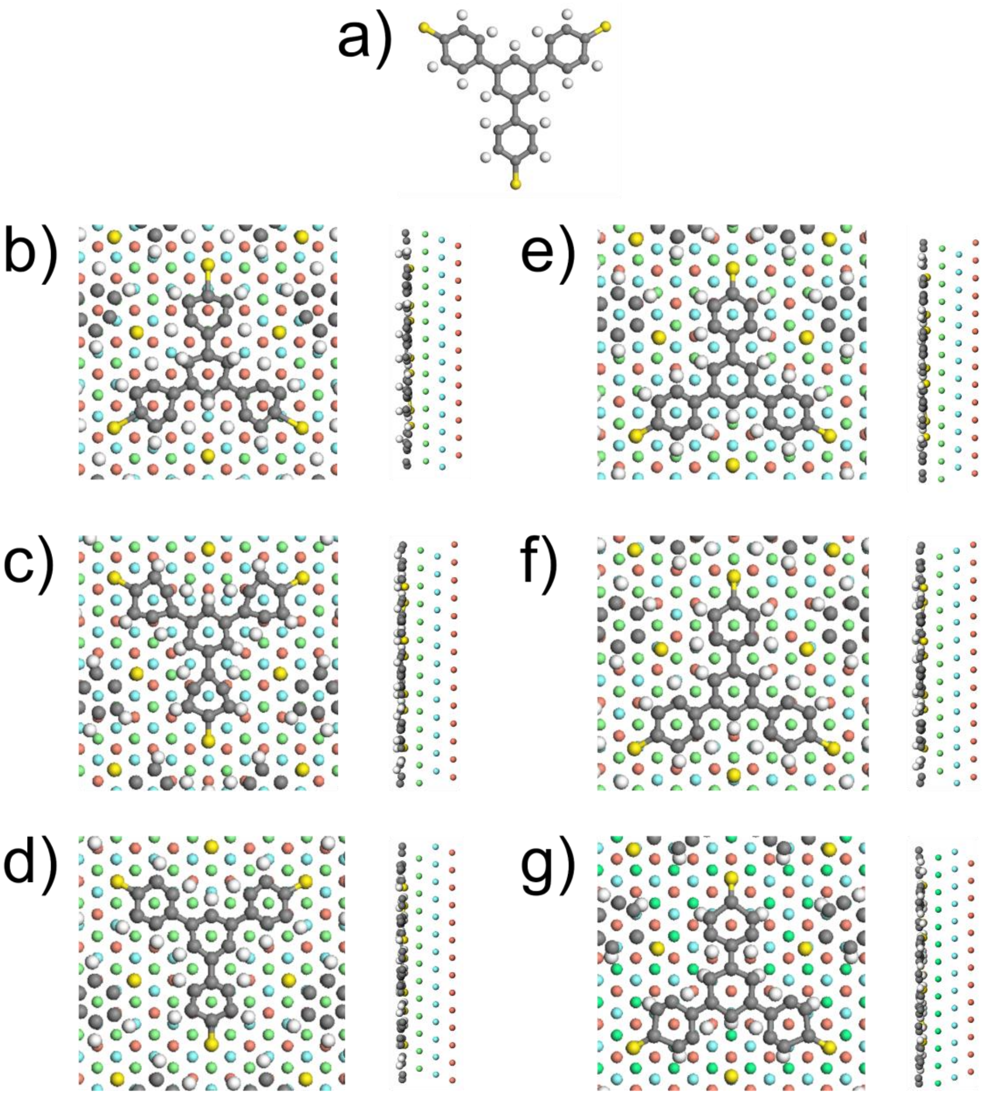

Supplementary Fig. S2 LEED optimization results for competing models. (a) Initial structure of TMB, *i.e.* before LEED structure optimization. (b)-(g) top- and side-view on the LEED optimized structures for all six symmetry-allowed adsorption geometries: (b) model 1, S: on top, phenyl: fcc; (c) model 2, S: on top, phenyl: hcp; (d) model 3, S: fcc, phenyl: on top; (e) model 4, S: fcc, phenyl: hcp; (f) model 5, S: hcp, phenyl: on top; (g) model 6, S: hcp, phenyl: fcc.

Intramolecular distances in TMB

Supplementary Table S2 Intramolecular distances in TMB. Comparison of DFT optimized structures of isolated TMB and the corresponding deprotonated trithiolate in the gas phase, as well as DFT optimized structures of the adsorbed trithiolate without or with dispersion correction, and LEED-optimized structure.

atoms	distance / pm				
	DFT				LEED-I(V)
	isolated trithiol	isolated trithiolate	TMB on Cu(111) without vdW	TMB on Cu(111) with vdW	
C1-C2	140	140	141	142	143
C2-C3	148	147	148	147	150
C3-C4	141	141	142	143	149
C4-C5	138	139	141	141	139
C5-C6	142	142	141	142	143
C6-S	170	173	178	179	176
C1-H1	108	109	108	109	113
C2-H2	109	109	110	109	110
C3-H3	109	109	109	109	110
S→S	1294	1300	1298	1302	1309
C1→S	885	891	895	898	903

Adsorption Heights: DFT without and with Dispersion Correction vs. LEED

Supplementary Table S3 Adsorption heights: Z-coordinates (in pm) of all adsorbate atoms with respect to the mean height of the upmost copper layer.

atom	**DFT (without vdW)**	**DFT (with vdW)**	**LEED-I(V)**
H1	303	248	270
H2	282	259	269
H3	247	237	269
C1	304	242	246
C2	304	243	254
C3	291	240	251
C4	276	238	246
C5	250	228	232
C6	233	217	228
S	198	200	201
mean all C-atoms	276	235	243
mean all atoms	269	235	247

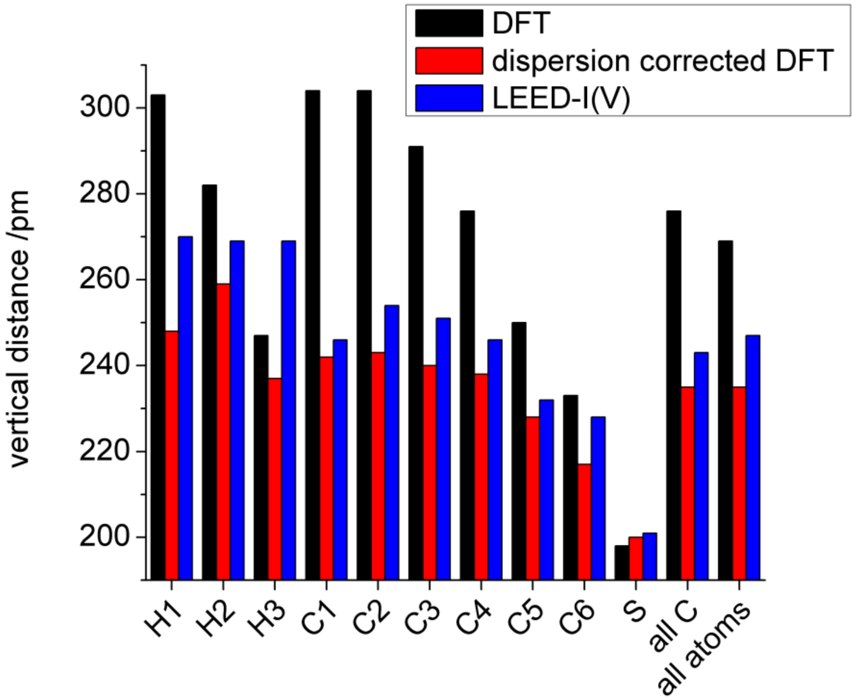

Supplementary Fig. S3 Visualization of the Z-Coordinates of Table S2.

Z-Coordinates of Selected Copper Atoms

Supplementary Table S4 Z-coordinates for selected copper atoms. LEED-I(V) and dispersion corrected DFT derived distances of selected sublayer copper atoms with respect to the mean height of the respective layer in pm. For copper atom labels cf. Fig. S4.

Atom	LEED-I(V)	DFT-vdW
Cu1	+ 10	+ 7
Cu2	- 1	- 3
Cu3	+ 3	- 1
Cu4	- 2	- 1

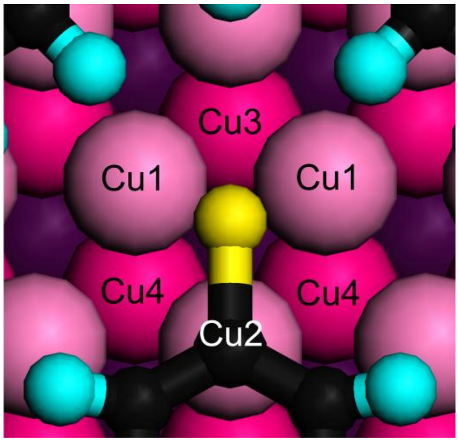

Supplementary Fig. S4 Labeling of selected copper atoms, displayed in Table S4.

Adatom-Based Models

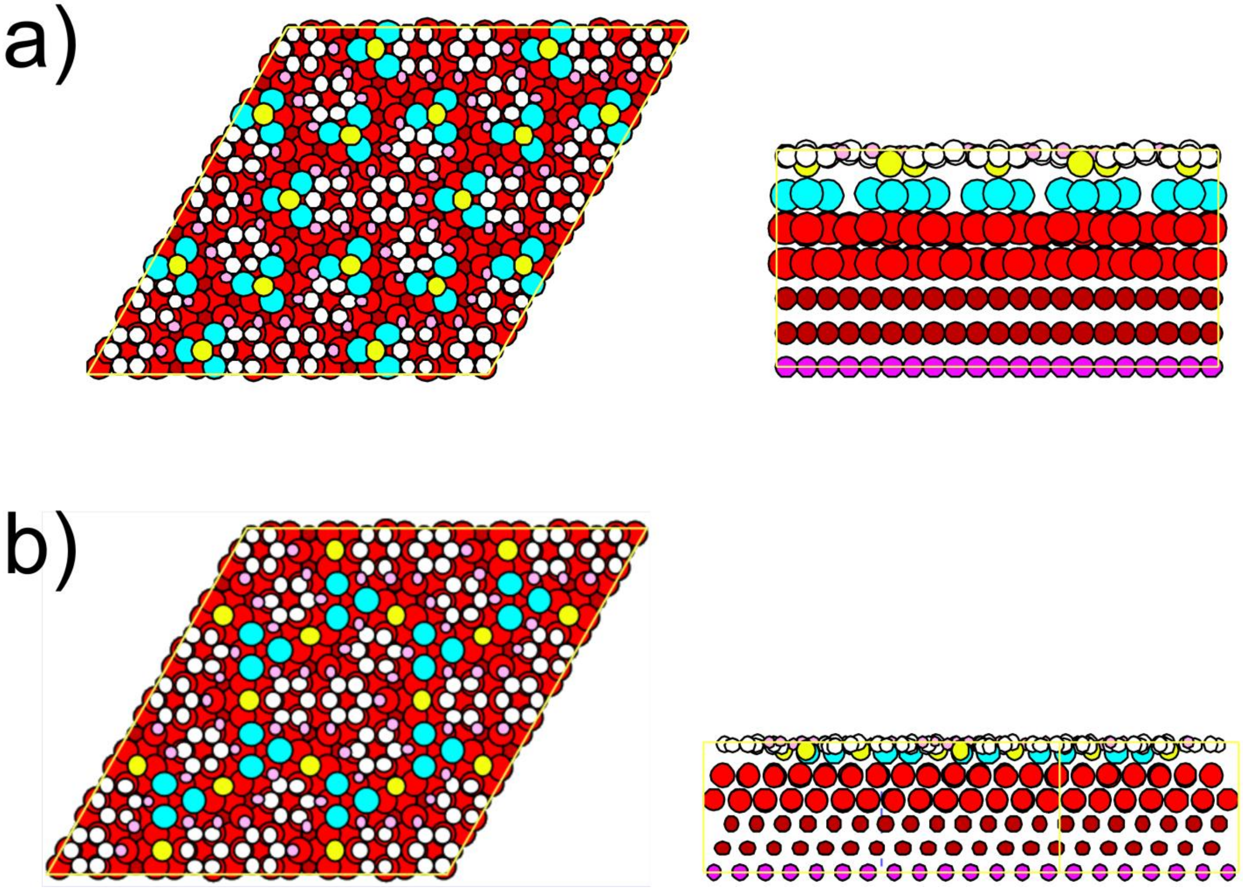

Supplementary Fig. S5 Adatom-based models, considered for the LEED-I(V) analysis. (a) adatom interlayer and (b) interstitial adatoms.

References

1 W. Moritz, *J. Phys. C Solid State*, 1984, **17**, 353-362.
2 G. Kleinle, W. Moritz and G. Ertl, *Surf. Sci.*, 1990, **238**, 119-131.
3 H. Over, U. Ketterl, W. Moritz and G. Ertl, *Phys. Rev. B*, 1992, **46**, 15438-15446.
4 H. Walch, J. Dienstmaier, G. Eder, R. Gutzler, S. Schlögl, T. Sirtl, K. Das, M. Schmittel and M. Lackinger, *J. Am. Chem. Soc.*, 2011, **133**, 7909-7915.
5 S. J. Clark, M. D. Segall, C. J. Pickard, P. J. Hasnip, M. J. Probert, K. Refson and M. C. Payne, *Z. Kristallogr.*, 2005, **220**, 567-570.
6 D. Vanderbilt, *Phys. Rev. B*, 1990, **41**, 7892-7895.
7 J. P. Perdew, K. Burke and M. Ernzerhof, *Phys. Rev. Lett.*, 1996, **77**, 3865-3868.
8 A. Tkatchenko and M. Scheffler, *Phys. Rev. Lett.*, 2009, **102**, 073005.
9 H. J. Monkhorst and J. D. Pack, *Phys. Rev. B*, 1976, **13**, 5188-5192.